

Catalytic Cracking, Dehydrogenation, and Aromatization of Isobutane over Ga/HZSM-5 and Zn/HZSM-5 at Low Pressures

YANPING SUN, TREVOR C. BROWN

Chemistry, University of New England, Armidale, NSW, 2351, Australia

Received 28 December 2001; accepted 17 April 2002

DOI 10.1002/kin.10073

ABSTRACT: Isobutane cracking, dehydrogenation, and aromatization over Ga/HZSM-5 and Zn/HZSM-5 has been investigated in a Knudsen cell reactor and the kinetics of the primary reaction steps for isobutene and propene formation have been accurately determined. Although cracking is the dominant reaction channel, with propene and methane being primary products, methane formation is significantly less than propene formation. This indicates that a proportion of the cracking proceeds via Lewis acid attack at C—C bonds, and not just via alkanium ion formation at Bronsted acid sites. This is particularly apparent over Zn/HZSM-5. Intrinsic rate constants for cracking, calculated from the rate of propene formation, are

$$k_{3a}(\text{°C}^{-1}) = 10^{18.3 \pm 1.1} \exp(-148 \pm 6 \text{ kJ mol}^{-1}/RT) \quad \text{Ga/HZSM-5}$$

$$k_{3a}(\text{°C}^{-1}) = 10^{14.8 \pm 1.1} \exp(-114 \pm 6 \text{ kJ mol}^{-1}/RT) \quad \text{Zn/HZSM-5}$$

and for dehydrogenation, calculated from the rate of isobutene formation, are

$$k_{3b}(\text{°C}^{-1}) = 10^{18.0 \pm 1.1} \exp(-148 \pm 6 \text{ kJ mol}^{-1}/RT) \quad \text{Ga/HZSM-5}$$

$$k_{3b}(\text{°C}^{-1}) = 10^{13.5 \pm 1.1} \exp(-101 \pm 6 \text{ kJ mol}^{-1}/RT) \quad \text{Zn/HZSM-5}$$

Large preexponential factors for cracking and dehydrogenation over Ga/HZSM-5 indicate that either the coverage of active sites is significantly less than the coverage of exposed sites or the

Correspondence to: Dr. Trevor Brown; e-mail: tbrown3@metz.une.edu.au.

Contract grant sponsor: Australian Research Council.
© 2002 Wiley Periodicals, Inc.

intrinsic reaction step involves a large entropy change between reactant and transition state. For Zn/HZSM-5 the small preexponential factors suggest either small entropy changes during activation, perhaps initiated by Lewis acid sites, or a steady-state distribution of active and exposed sites is rapidly reached. Differences in intrinsic activation energies may reflect the ratio of Lewis and Bronsted acid sites on the respective catalyst surfaces. Aromatization is more prolific over Ga/HZSM-5 than over Zn/HZSM-5 under the low-pressure conditions. © 2002 Wiley Periodicals, Inc. *Int J Chem Kinet* 34: 467–480, 2002

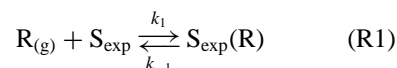
INTRODUCTION

Aromatization rates of small alkanes over HZSM-5 are greatly enhanced by the introduction of gallium or zinc cations. For industrial applications Ga-containing zeolites are generally preferred over Zn/HZSM-5 for alkane aromatization as zinc is eluted from the latter catalyst during alkane conversion [1–3]. Over pure HZSM-5, cracking and dehydrogenation are the dominant reaction pathways. At low temperatures these decomposition steps are initiated by proton donation from the pure zeolite to the alkane to form highly energetic alkanium ions [4]. A number of studies have aimed to determine the role of ion exchanged or impregnated metal cations in cracking, dehydrogenation and aromatization. The experimental evidence suggests that both zinc and gallium species are either directly or indirectly responsible for increasing the rate of dehydrogenation of the alkane reactant [5]. One proposal is that hydride abstraction in the vicinity of Ga [6] and Zn [7] sites is the initial rate-determining step. Others have concluded that Zn and Ga cations are the driving force for dehydrogenation by combining the H-atoms, which form during the activation of C–H at Bronsted acid sites [8]. This occurs by the cyclic reduction and oxidation of Zn and Ga species [9]. All other reaction steps occur on Bronsted acid sites within the zeolite micropores, [5] although it has been suggested that zinc may also be involved in oligomerization of the alkenium ions and dehydrogenation of cycloalkenes [7].

In this paper the kinetics of the initial steps in the catalytic cracking, dehydrogenation, and aromatization of isobutane over Ga/HZSM-5 and Zn/HZSM-5 have been investigated in a Knudsen cell reactor. Under low-pressure conditions the first steps in a heterogeneous reaction can generally be observed because gas-phase and surface bimolecular reactions are minimized. Furthermore this technique allows for the determination of accurate rate parameters as the gas/surface collision frequency may be accurately calculated and can be varied by either adjusting the flow rate, the exposed surface area of the catalyst, or the exit aperture area [4]. Also by including temperature programming, temperature-fluctuations resulting from nonequilibrium adsorption

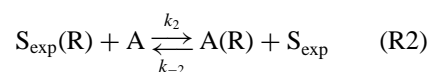
on clean surfaces are minimized and a range of temperatures can be investigated over a short period of time, without an internal standard. Although these techniques have the effect of minimizing both secondary reactions and heat fluctuations the likely reaction scheme remains complex, as it involves several steps:

- (i) Adsorption of gas-phase reactant R on the exposed surface of the catalyst S_{exp}

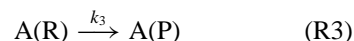


Direct adsorption onto active sites is not included, as most of the catalytic activity is within the micropores of the zeolite structure.

- (ii) Reactant surface diffusion to and from active sites A



- (iii) Intrinsic reaction at the active sites to form adsorbed products A(P)

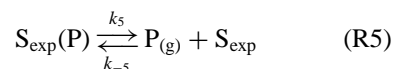


This step may also involve several steps, such as alkanium ion formation, rearrangement to alkenium ions and formation of alkenes.

- (iv) Product diffusion from active sites to the exposed surface



- (v) Product desorption from the exposed surface



- (vi) Escape from the Knudsen cell through the exit aperture with rate constant k_{ep}



As a first approximation it is assumed that steps (R1) and (R3) are rate determining. This means that a steady state is quickly reached between the coverage of the exposed and active sites (step (R2)), and that adsorbate diffusion (step (R3)) and desorption (step (R5)) are rapid. Also the escape rate constant k_{ep} must be significantly larger than the intrinsic rate constant k_3 . Larger than expected Arrhenius preexponential factors for the intrinsic cracking and dehydrogenation of isobutane over HZSM-5 have been previously attributed to an inequality in the coverage of exposed and active sites [4].

EXPERIMENTAL

The Knudsen cell reaction system has been described in detail elsewhere [4]. Briefly, isobutane passes through a variable leak valve (Granville–Phillips), through 240 mm of 1 mm ID capillary glass tubing and into the Pyrex reaction cell containing the solid substrate. Reactant molecules then experience collisions with the walls of the reactor and substrate, prior to escaping through the exit aperture and directly into a quadrupole mass spectrometer. Reactor and substrate geometry determine the average number of collisions within the Knudsen cell. Flow rate is monitored before each experiment by recording the pressure decrease from the pressure gauge situated, in a known volume, next to the variable leak valve. The detection system is a Hewlett Packard 5995 quadrupole mass spectrometer. Details of the two reactors used in the analysis are listed in Table I. Collision numbers (Z) are calculated from the

Table I Key Physical Parameters, Calculated in the Absence of a Catalyst, for the Two Knudsen Cell Reactors

	Reactor 1	Reactor 2
Volume	$8830 \pm 5 \text{ mm}^3$	$7414 \pm 5 \text{ mm}^3$
Internal surface area	$2355 \pm 2 \text{ mm}^2$	$2320 \pm 2 \text{ mm}^2$
Exit aperture area	$0.95 \pm 0.03 \text{ mm}^2$	$1.54 \pm 0.03 \text{ mm}^2$
Collisions/molecule	2480 ± 200	1510 ± 200
Residence time (s)	$0.25(M/T)^{1/2}$	$0.13(M/T)^{1/2}$

ratio of the area of the reactor walls (S_v) to the area of the exit aperture (S_{ea}). Measured exit aperture areas can be corrected by Clausing factors [10] to take into account the finite width of the exit aperture, but for the current reactors this factor is estimated to be one.

Zeolyst International (Kansas City, USA) supplied the ammonium ZSM-5 powder (CBV 3024G) and conversion to HZSM-5 was achieved by heating in air at 500°C. The original zeolite has a unit cell formula of $\text{NH}_{5.48}(\text{Si}_{90.52}\text{Al}_{5.48})\text{O}_{190.9}$ and N_2 BET surface area of $400 \pm 10 \text{ m}^2 \text{ g}^{-1}$. Zn/HZSM-5 and Ga/HZSM-5 were prepared by ion exchange with HZSM-5 at 343 K for 24 h in solutions of either 0.0050 M zinc nitrate or 0.0050 M gallium nitrate. The exchanged zeolites were then dried in flowing air at 383 K for 24 h and then at 773 K for another 24 h. All substrates were pressed binder-free and crushed to particles of 0.15–0.23 mesh size. The Ga and Zn content was determined by X-ray fluorescence and found to be 0.5 wt% in both cases. X-ray diffraction patterns for pure HZSM-5, Zn/HZSM-5 and Ga/HZSM-5 were similar. This indicated that the metals are finely dispersed and that no dealumination or damage to the zeolite structure has occurred during ion exchange. Isobutane, isobutene, propene, methane, benzene, toluene, and xylene were used as supplied without further purification.

RESULTS

Temperature Programmed Reaction Profiles

A careful analysis of the mass spectra that resulted from the exposure of isobutane to Zn/HZSM-5 and Ga/HZSM-5 at temperatures ranging from 200 to 500°C indicated that the only products were methane, propene, isobutene, benzene, toluene, and xylene (molecular hydrogen could not be accurately detected). Small amounts of ethene could also be evolved, particularly over Ga/HZSM-5, but quantification was difficult because of the interference of characteristic mass spectral peaks from major products. Other possible products, ethane, propane, *n*-butanes, and pentanes were not observed. When isobutane was flowed through the reaction cell in the absence of catalyst no reaction was apparent over the temperature range. For the kinetic analysis gas-phase species were characterized by $m/e = 13$ (methane), $m/e = 36$ (propene), $m/e = 56$ (isobutene), $m/e = 58$ (isobutane), $m/e = 78$ (benzene), $m/e = 91$ (toluene), and $m/e = 106$ (xylene). Isobutane had peaks at $m/e = 56$, $m/e = 36$, and $m/e = 13$, which were measured at the commencement of each temperature program when no reaction was

apparent. Isobutene had peaks at $m/e = 36$ and $m/e = 13$, while propene contributed to $m/e = 13$. For the aromatics xylene had peaks at $m/e = 91$ and $m/e = 78$, while toluene contributed to $m/e = 78$. For these products calibration factors were determined using the pure gas or vapor over a range of flow rates. These are listed in Table II. Also listed are mass-spectral conversion factors (α (abundance s molecule⁻¹)), which convert flow rate to abundance for the gaseous species. Accurate conversion factors for benzene, toluene, and xylene could be easily determined because a broad range of vapor flow rates was difficult to control and measure. Hence, conversion factors for each of the aromatics were calculated from a reactant and product mass balance.

$$\begin{aligned} & \frac{(I_{C_4H_{10}}^{\circ} - I_{C_4H_{10}})}{\alpha_{C_4H_{10}}} - \frac{I_{C_4H_8}}{\alpha_{C_4H_8}} - \frac{I_{C_3H_6}}{\alpha_{C_3H_6}} \\ &= 2 \left(\frac{I_{Benzene}}{\alpha_{Benzene}} + \frac{I_{Toluene}}{\alpha_{Toluene}} + \frac{I_{Xylene}}{\alpha_{Xylene}} \right) \end{aligned} \quad (1)$$

where $I_{C_4H_{10}}^{\circ}$ and $I_{C_4H_{10}}$ are mass-spectral abundances characteristic of isobutane before and after reaction, respectively. Rearranging leads to the following expression for calculating the conversion factor for benzene

$$\alpha_{Benzene} = \frac{2(I_{Benzene} + \frac{I_{Toluene}}{a} + \frac{I_{Xylene}}{a'})}{\frac{(I^{\circ} - I)}{\alpha_{C_4H_{10}}} - \frac{I_{C_4H_8}}{\alpha_{C_4H_8}} - \frac{I_{C_3H_6}}{\alpha_{C_3H_6}}} \quad (2)$$

The two experimentally measured constants a and a' are the ratios of calibration constants $\alpha_{Toluene}/\alpha_{Benzene}$ and $\alpha_{Xylene}/\alpha_{Benzene}$, respectively. For toluene $a = 0.50 \pm 0.05$ and for *p*-xylene $a' = 0.30 \pm 0.05$.

Eight temperature-programmed experiments were carried out for isobutane flowing over Zn/HZSM-5 and Ga/HZSM-5. Flow rates ranged from 2.16×10^{14} to 2.90×10^{15} molecules s⁻¹ (isobutane reactor pressure ranged from 1–20 Pa) and the heating rate was varied between 2 and 5°C min⁻¹. For 5°C min⁻¹ the heating

rate became nonlinear between 490 and 500°C and so, for kinetic analysis, data in this region were discarded. Typical profiles for isobutane over Ga/HZSM-5 and Zn/HZSM-5 are plotted in Figs. 1 and 2. Here the heating rate is 5°C min⁻¹ and flow rates into the reactor were 4.73×10^{14} and 5.61×10^{14} molecules s⁻¹ respectively. For both substrates the isobutane escape rate continuously declined from ~300°C, while products began to appear from this temperature. Because of different reactant and product sensitivities to the characteristic mass spectral peaks, more informative profiles were obtained by plotting fractional yield and decomposition against temperature. Fractional decomposition of isobutane and fractional yields of products were calculated from

$$f_{Decomposition} = \frac{I_{C_4H_{10}}^{\circ} - I_{C_4H_{10}}}{I_{C_4H_{10}}^{\circ}} \quad (3)$$

$$f_{Yield} = \frac{\alpha_{C_4H_{10}} I_{Product}}{\alpha_{Product} I_{C_4H_{10}}^{\circ}} \quad (4)$$

and are plotted in Figs. 3–6. Only 60% of isobutane decomposed over Zn/HZSM-5 at 500°C, while under similar conditions almost 90% was lost over Ga/HZSM-5. Product evolution rates decreased in the order propene > isobutene > methane > benzene > toluene > xylene for Zn/HZSM-5 catalysis and propene > methane > isobutene ≈ toluene > benzene > xylene for Ga/HZSM-5. That is, for both systems propene was the dominant product and xylene had the lowest yield, while evolution order for the other four products was dependent on the catalyst. Propene was also the dominant product for isobutane decomposition over pure HZSM-5 [4].

Kinetics of Alkane and Alkene Formation

The methodology used to determine rate parameters for alkane and alkene formation during cracking and dehydrogenation has been previously described in

Table II Calibration Factors for the Mass Spectrometer

	α (I s mol ⁻¹)	Corrected Abundance
Isobutane	$(1.2 \pm 0.2) \times 10^{14}$	I_{58}
Isobutene	$(1.8 \pm 0.6) \times 10^{15}$	$I_{56} = I_{56} - (0.138 \pm 0.003) \times I_{58}$
Propene	$(4.2 \pm 0.5) \times 10^{13}$	$I_{36} = I_{36} - (0.0461 \pm 0.0017) \times I_{58} - (0.0115 \pm 0.0011) \times I_{56}$
Methane	$(1.6 \pm 0.1) \times 10^{14}$	$I_{13} = I_{13} - (0.00610 \pm 0.0008) \times I_{58} - (0.009 \pm 0.003) \times I_{56} - (0.49 \pm 0.03) \times I_{36}$
Benzene	$(3.0 \pm 0.9) \times 10^{15}$	$I_{78} = I_{78} - (0.162 \pm 0.003) \times I_{106} - (0.0026 \pm 0.0005) \times I_{91}$
Toluene	$(1.5 \pm 0.4) \times 10^{15}$	$I_{91} = I_{91} - (2.11 \pm 0.18) \times I_{106}$
Xylene	$(8.9 \pm 0.3) \times 10^{14}$	I_{106}

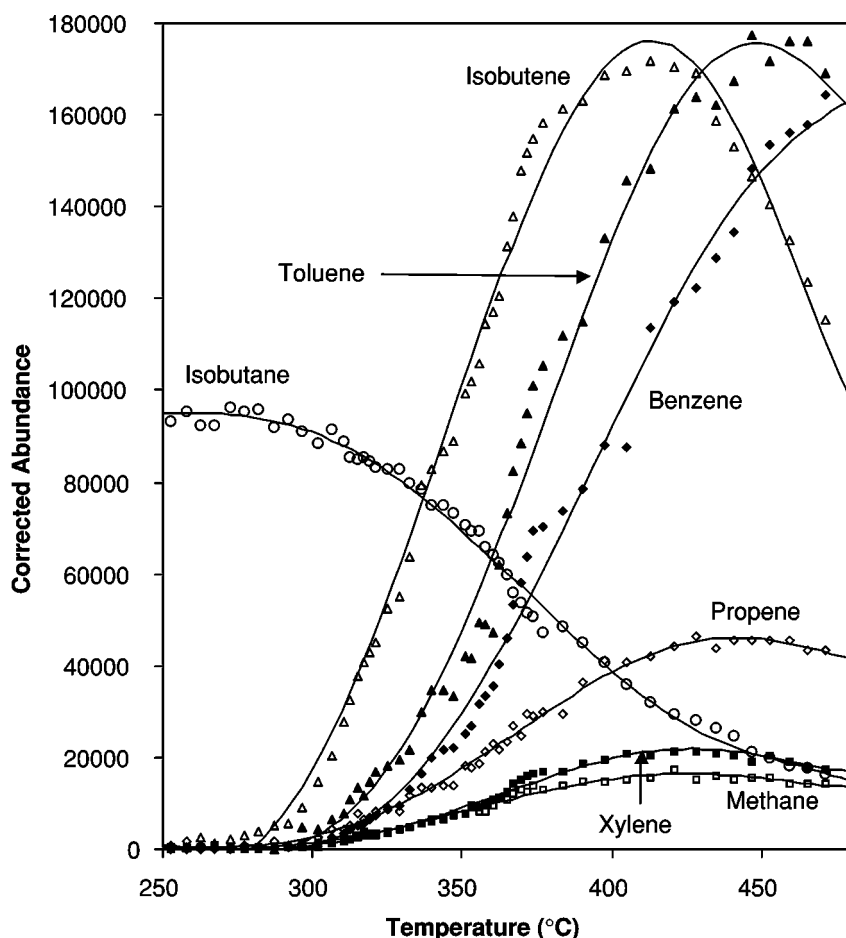
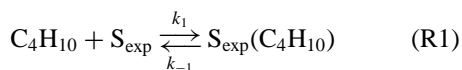


Figure 1 Corrected mass-spectral abundances for Ga/HZSM-5 decomposition of isobutane (\circ $m/e = 58$), formation of isobutene (Δ $m/e = 56$), propene (\diamond $m/e = 36$), methane (\square $m/e = 13$), and aromatics as indicated, during temperature programming. Initial isobutane flow rate is 4.73×10^{14} molecules s^{-1} and heating rate is $5^\circ C \text{ min}^{-1}$.

detail [4]. Assumed rate determining steps are adsorption and desorption of isobutane and surface reaction.



Here adsorbed species are in parentheses. The rate constants k_{-1} , k_{3a} , and k_{3b} have units $s^{-1} \text{ site}^{-1}$, while $k_1 P_{C_4H_{10}}$, where P is partial pressure, is the isobutane/catalyst surface collision frequency. Rate constants for surface diffusion to or from active sites have been previously estimated to be of the order $4 \times 10^6 - 3 \times 10^9 s^{-1}$ [4] and so as a first approximation these steps are considered not to be rate determining. The

abundance of a mass spectral peak uniquely characteristic of a primary product is proportional to the mass-spectral calibration factor and the product flow rate,

$$I_{\text{Product}} = \alpha_{\text{Product}} \frac{dn_{\text{Product}}}{dt} \quad (5)$$

The product flow rate may be calculated from the collision number Z , the average reactant flow rate and a ratio of rate constants determined by assuming a steady-state coverage of isobutane:

$$\frac{dn_{\text{Product}}}{dt} = \frac{k_{3a \text{ or } 3b}}{k_{-1} + k_{3a} + k_{3b}} Z \frac{dn_{C_4H_{10}}}{dt} \quad (6)$$

The collision number is the ratio of the exposed catalyst surface area to the exit aperture area ($S_{\text{HZ,e}}/S_{\text{ea}}$), while the reactant flow rate is calculated from the mean of the

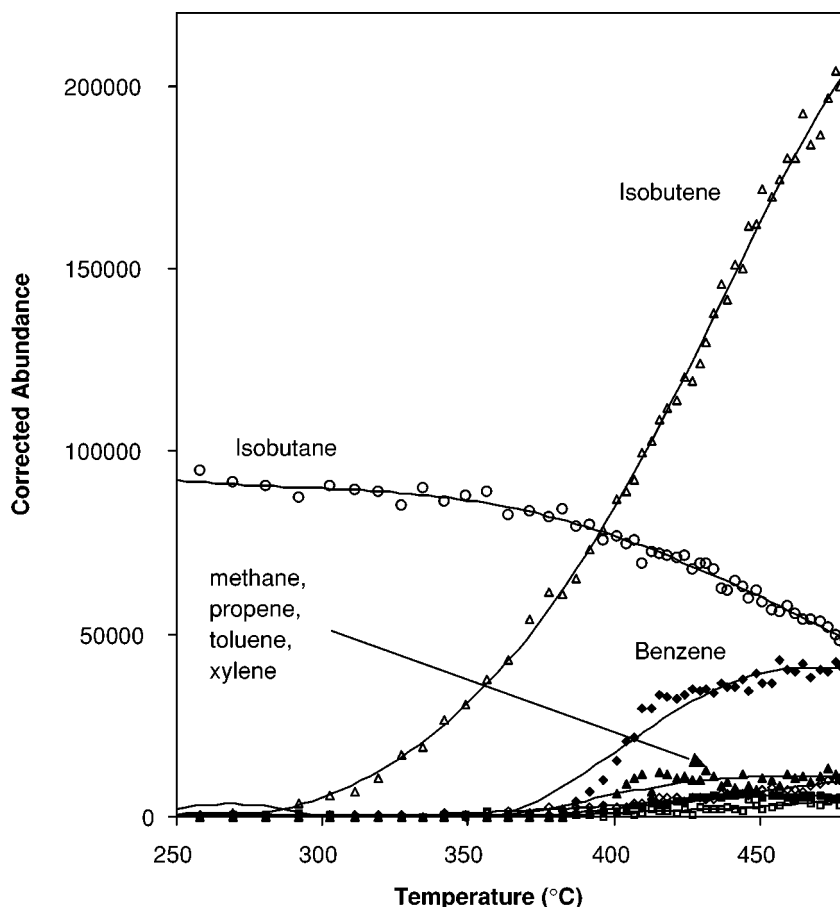


Figure 2 Corrected mass-spectral abundances for Zn/HZSM-5 catalyzed decomposition of isobutane (\circ $m/e = 58$), formation of isobutene (Δ $m/e = 56$), propene (\diamond $m/e = 36$), methane (\square $m/e = 13$), and aromatics as indicated, during temperature programming. Initial isobutane flow rate is 5.61×10^{14} molecules s^{-1} and heating rate is 5°C min^{-1} .

abundances entering and leaving the Knudsen cell

$$I_{\text{Product}} = \frac{\alpha_{\text{Product}} S_{\text{HZ,e}} k_{3a \text{ or } 3b} \exp\left(\frac{-E_1}{RT}\right)}{\alpha_{\text{C}_4\text{H}_{10}} S_{\text{ea}} (k_{-1} + k_{3a} + k_{3b})} \times \frac{(I_{\text{C}_4\text{H}_{10}}^\circ + I_{\text{C}_4\text{H}_{10}})}{2} \quad (7)$$

The activation energy for adsorption (E_1) of isobutane onto the zeolite surface was included in these calculations. The geometric surface area of the catalyst [11,12] was used as an estimate for the exposed surface area of the catalyst and could have introduced errors of a factor of ten in the reported Arrhenius preexponential factors. A value of 330 mm^2 for $S_{\text{HZ,e}}$ was used in all calculations, which represents ca. 14% of the internal surface area of the Knudsen cell reactor. Further simplification of Eq. (7) is possible by noting that the surface reaction rate constants (k_{3a}) and (k_{3b}) are much smaller than the isobutane desorption rate constant (k_{-1}). Hence the full rate expression with Arrhenius parameters for each

surface reaction step is

$$I_{\text{Product}} = \frac{\alpha_{\text{Product}} S_{\text{HZ,e}} A_{3a \text{ or } 3b}}{\alpha_{\text{C}_4\text{H}_{10}} S_{\text{ea}} A_{-1}} \times \exp\left(\frac{-E_1 + E_{-1} - E_{3a \text{ or } 3b}}{RT}\right) \times \frac{(I_{\text{C}_4\text{H}_{10}}^\circ + I_{\text{C}_4\text{H}_{10}})}{2} \quad (8)$$

The unknowns in this expression are the preexponential factors and activation energies. These are determined by taking the natural logarithm of Eq. (8) and rearranged to give

$$\ln\left(\frac{(I_{\text{C}_4\text{H}_{10}}^\circ + I_{\text{C}_4\text{H}_{10}}) \alpha_{\text{Product}} S_{\text{HZ,e}}}{2 I_{\text{Product}} \alpha_{\text{C}_4\text{H}_{10}} S_{\text{ea}}}\right) = \ln\left(\frac{A_{-1}}{A_{3a \text{ or } 3b}}\right) + \left(\frac{E_1 - E_{-1} + E_{3a \text{ or } 3b}}{RT}\right) \quad (9)$$

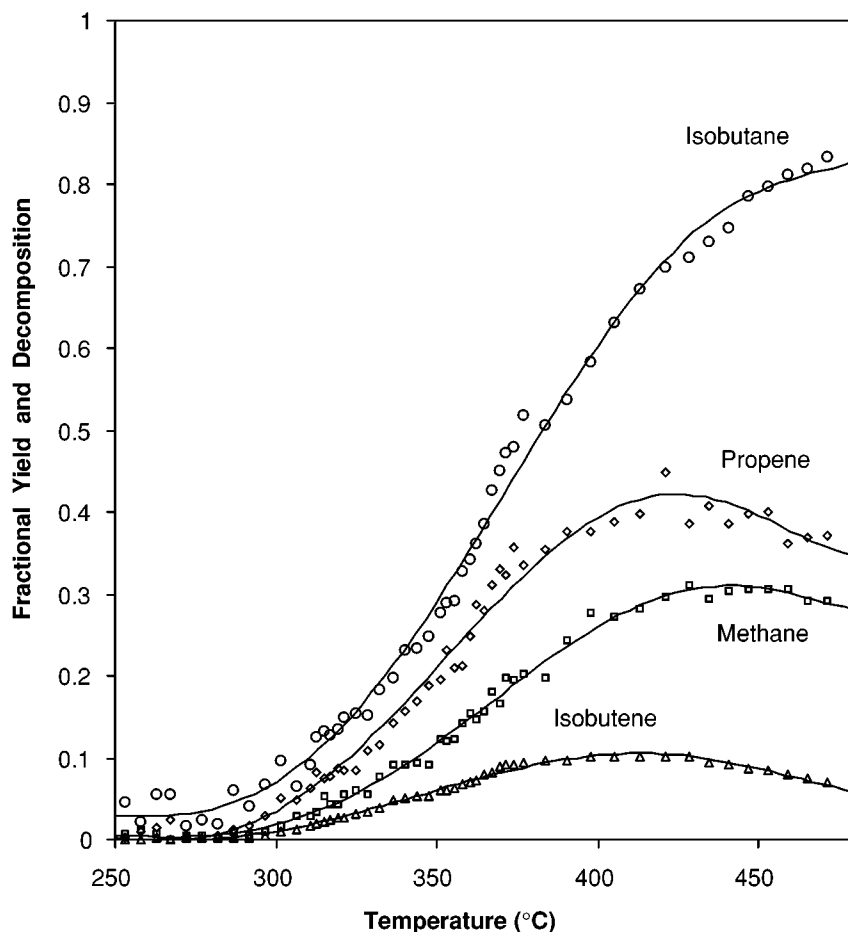


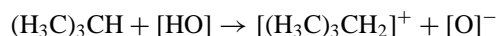
Figure 3 Fractional isobutane decomposition (\circ) over Ga/HZSM-5 and apparent yields of isobutene (Δ), propene (\diamond) and methane (\square), calculated from abundances plotted in Fig. 1.

A plot of the left-hand side of Eq. (9) against $1/RT$ produced a straight line with slope equal to $E_1 - E_{-1} + E_{3a}$ or $3b$ and an intercept of $\ln(A_{-1}/A_{3a}$ or $3b)$. This plot is shown in Figs. 7 and 8 for the temperature-programmed experiments depicted in Figs. 1 and 2. For all Arrhenius plots overall conversions of 10–50% were used. Average Arrhenius preexponential factors and activation energies with standard deviations determined from all temperature-programmed isobutane decompositions over Ga/HZSM-5 and Zn/HZSM-5 systems are listed in Table III.

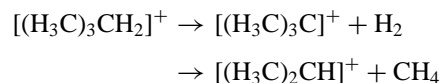
DISCUSSION

The observations of particular significance in the temperature-programmed reaction profiles obtained for both catalysts are the low yields of methane (Figs. 3 and 5). In the case of isobutane cracking over Ga/HZSM-5 the ratio of propene to methane was ca. 2:1 while for Zn/HZSM-5 the ratio was ca. 8:1. For

isobutane cracking over pure HZSM-5 this ratio was less than 2:1, which is not considered to be significant [4]. In this system it was assumed that the intrinsic reaction step is dominated by the formation of alkanium ions $[(H_3C)_3CH_2]^+$ at Bronsted sites [HO]



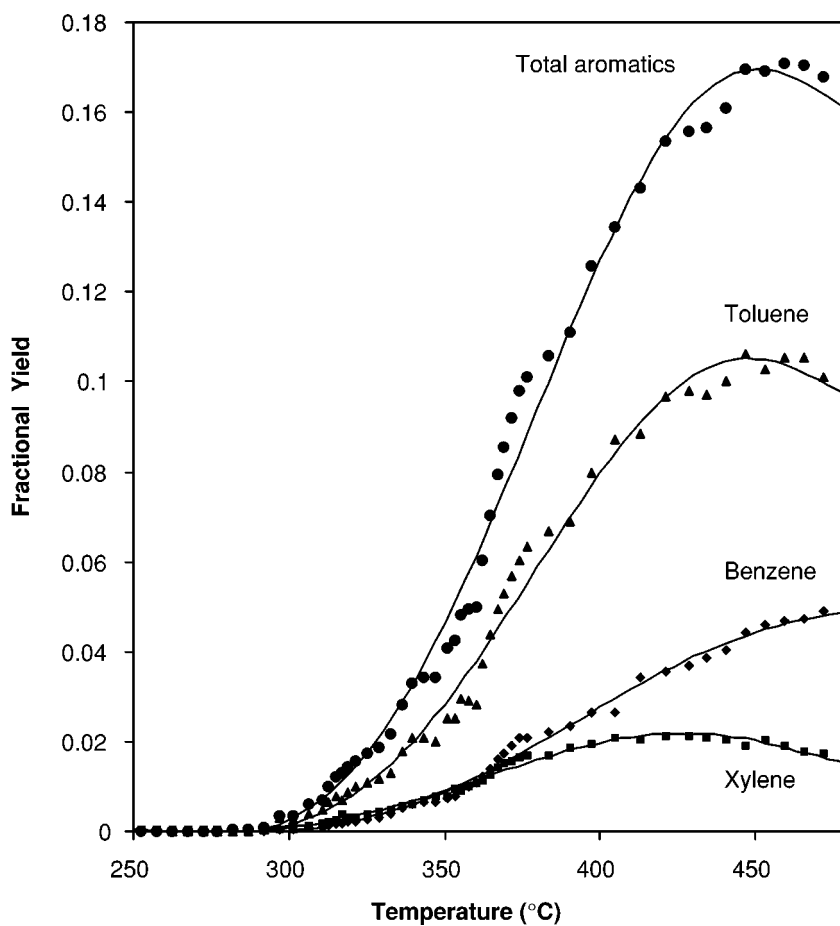
which subsequently rearrange to alkenium ions releasing hydrogen and methane.



It is then assumed that the molecular species proceed to the mass spectrometer, while the alkenium ions rapidly eliminate a proton to form propene or isobutene. However, as yields of methane are low over all HZSM-5 catalysts, particularly Zn/HZSM-5, a different mechanism must be invoked. In this case the rate determining

Table III Measured Arrhenius Rate Parameters for the Cracking and Dehydrogenation of Isobutane Over HZSM-5 [4], Ga/HZSM-5 and Zn/HZSM-5. Preexponential Factors have been Adjusted for the Heating Rate β

	Apparent		Intrinsic	
	$\log(\beta A_{-1}/A_3)$ ($\log(^{\circ}\text{C s}^{-1})$)	$E_1 - E_{-1} + E_3$ (kJ mol^{-1})	$\log(A_3/\beta)$ ($\log(^{\circ}\text{C}^{-1})$)	E_3 (kJ mol^{-1})
HZSM-5				
Cracking	-5.30 (12)	121.7 (1.7)	17.3 (1.1)	170 (6)
Dehydrogenation	-4.81 (12)	123.4 (1.7)	16.8 (1.1)	172 (6)
Ga/HZSM-5				
Cracking	-5.72 (12)	93.3 (1.6)		
Corrected ^a	-6.29 (12)	99.1 (1.4)	18.3 (1.1)	148 (6)
Dehydrogenation	-4.80 (10)	88.7 (1.2)		
Corrected ^a	-5.96 (10)	99.6 (1.2)	18.0 (1.1)	148 (6)
Zn/HZSM-5				
Cracking	-2.85 (8)	67.3 (1.2)		
Corrected ^a	-2.76 (8)	65.7 (1.2)	14.8 (1.1)	114 (6)
Dehydrogenation	-1.60 (8)	53.6 (1.2)		
Corrected ^a	-1.54 (8)	52.5 (1.2)	13.5 (1.1)	101 (6)

^aCorrected parameters to account for the loss of alkenes to form aromatics.**Figure 4** Fractional apparent yields over Ga/HZSM-5 of toluene, benzene, and xylene calculated from the corrected abundances plotted in Fig. 1.

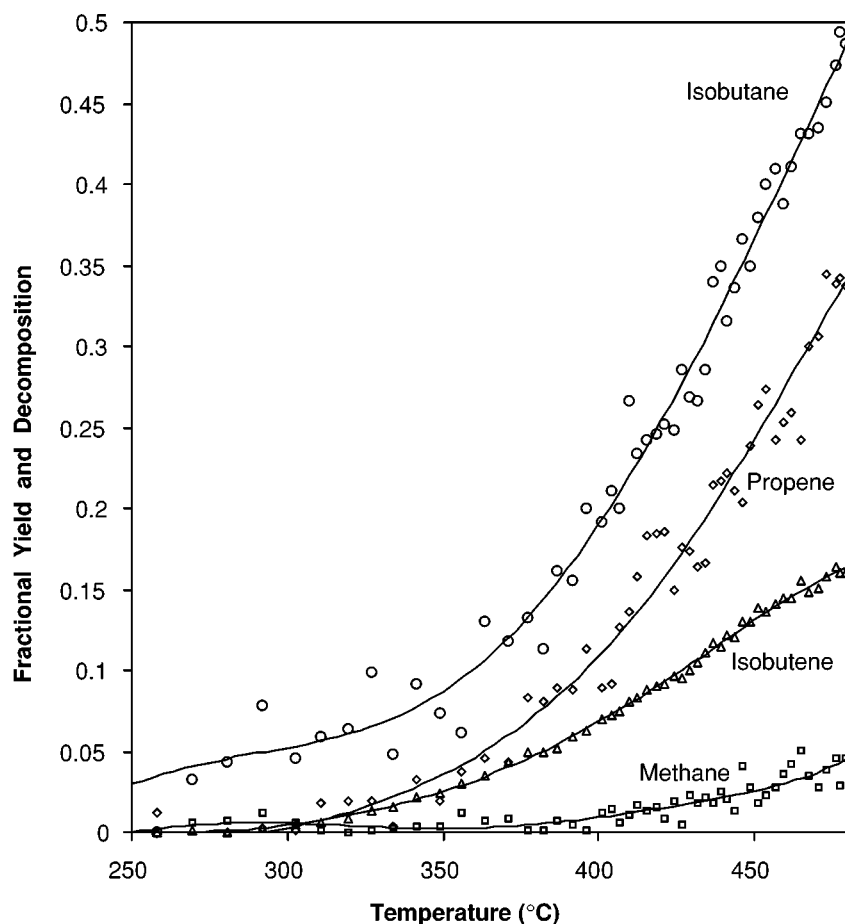
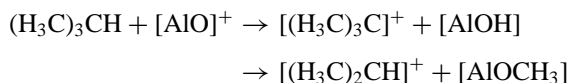


Figure 5 Fractional isobutane decomposition (\circ) over Zn/HZSM-5 and apparent yields of isobutene (Δ), propene (\diamond), and methane (\square), calculated from abundances plotted in Fig. 2.

step may be associated with zeolite Lewis acid sites $[\text{AlO}]^+$ or the added metal sites [6] where extraction of hydride ions and electron attack of C—C bonds can occur [13]. For example,



The hydrogen and methyl groups are bonded to the surface and can only desorb as molecular hydrogen or methane if they subsequently come into contact with a proton. Recombinative desorption of H-atoms as H_2 has been shown to occur at Zn and Ga cations [8]. Under low-pressure conditions H-atom coverage will be low and so recombination may be limited. As a consequence the effective rates of CH_4 and H_2 diffusion and desorption (steps (R4) and (R5)) may be rate determining.

An alternative to this proposed mechanism to explain the low methane yields is that a bimolecular

initiating step is dominant. Bimolecular surface processes are already apparent with the formation of aromatics over both Ga/HZSM-5 and Zn/HZSM-5. For isobutane transformations over H-mordenite it has been demonstrated that the primary products are propane, *n*-butane and isopentane, involving the formation of a C_8 alkenium ion; methane is not a major product [14]. Over the two HZSM-5 catalysts the only observed primary products from the Knudsen cell are methane, propene and isobutene. Hence it is unlikely that a bimolecular step is the dominant initiating reaction step for cracking and dehydrogenation, and so does not explain the observed low yield of methane.

Cracking, Dehydrogenation, and Aromatization over Ga/HZSM-5

From Fig. 1 it is apparent that after an initial exponential increase product evolution rates begin to plateau at about 370°C or 50% conversion. This slowing of

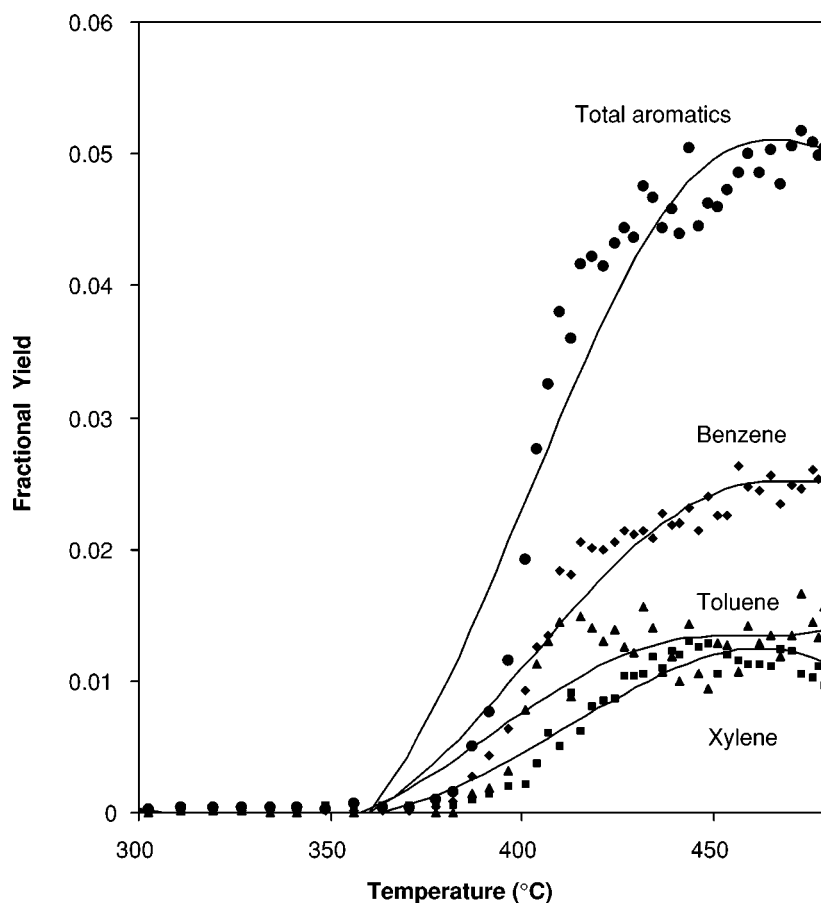


Figure 6 Fractional apparent yields over Zn/HZSM-5 of toluene, benzene, and xylene calculated from the corrected abundances plotted in Fig. 2.

the change in rate is because isobutane pressure has decreased to a point where adsorption and transport to active sites is rate limiting. The decline is also due to the formation of aromatics. Temperature-dependent fractional yields shown in Fig. 4 indicate that the ratio of toluene to benzene is approximately 2:1, while toluene to xylene is 2:1 at low temperatures but increases to 5:1 at 500°C. Statistically the maximum ratio is 2:1 if the aromatics are produced from only two alkene precursors; isobutene and propene or related adsorbed complexes. That is, one isobutene and one propene molecule interact to give toluene, two isobutenes give xylene and two propenes give benzene. For xylene further decomposition to toluene and to benzene may be affecting the measured ratios at higher temperatures. It is reasonable to assume that surface alkenes or associated alkenium ions are precursors to aromatic formation [8].

Evolution rates of isobutene and propene must therefore be corrected to account for the loss due to aromatic formation. This is achieved by adjusting $\alpha_{\text{Product}}/I_{\text{Product}}$

in Eq. (9) according to

$$\frac{\alpha_{\text{Propene}}}{I_{\text{Propene},c}} = \frac{1}{\left(\frac{I_{\text{Propene}}}{\alpha_{\text{Propene}}} + \frac{2I_{\text{Benzene}}}{\alpha_{\text{Benzene}}} + \frac{I_{\text{Toluene}}}{\alpha_{\text{Toluene}}}\right)} \quad (10)$$

Benzene contributions are doubled because two propene molecules are lost to benzene formation. Analogous corrections were applied to the isobutene abundance to obtain adjusted rate parameters (Table III). The result was that the activation energy for isobutene formation increased by 10.8 kJ mol⁻¹ and propene formation increased by 5.8 kJ mol⁻¹. Preexponential factors for both pathways also increased. Corrections could also be applied to methane formation, as the conversion of xylene to toluene possibly included the release of methane. However, the correction was small and could not be accurately measured.

Apparent activation energies for cracking (propene formation) and dehydrogenation (isobutene formation) over Ga/HZSM-5 were similar. This was also the case

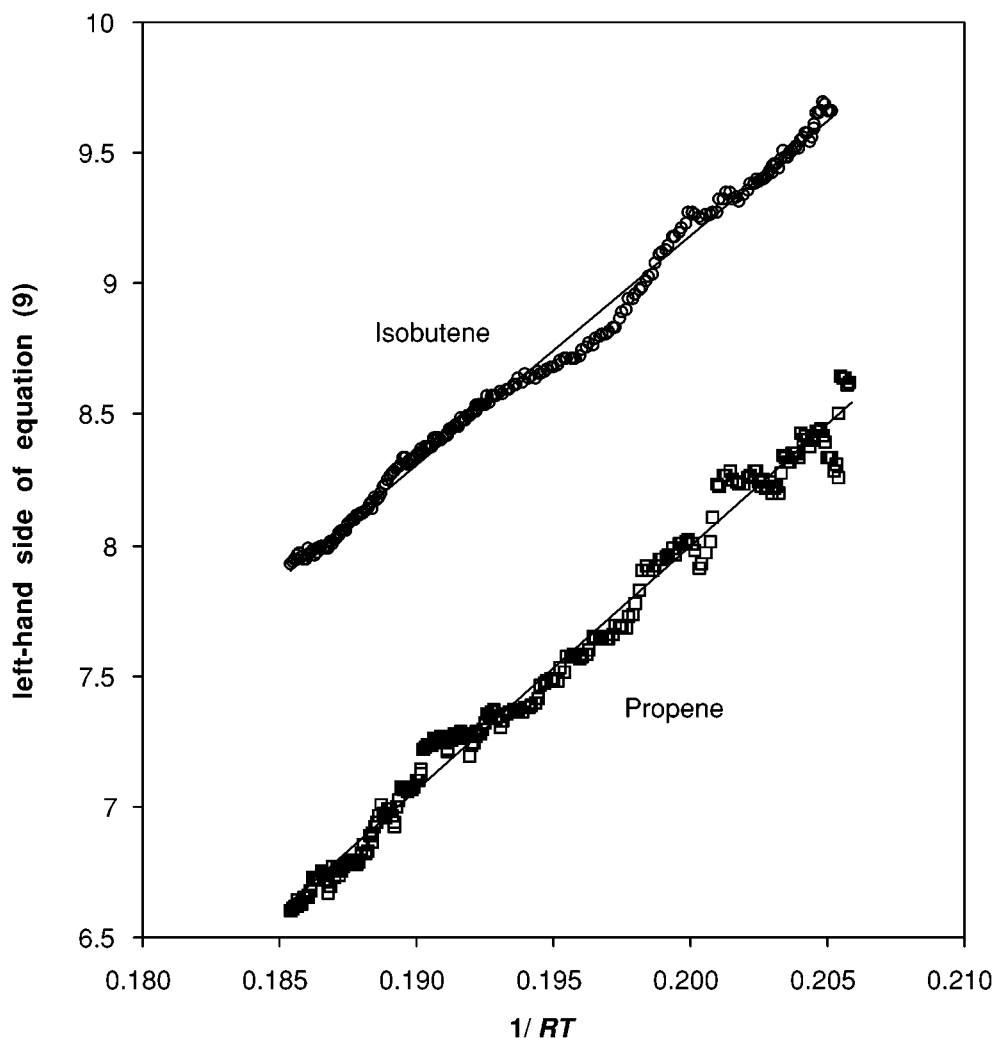


Figure 7 Arrhenius-type plots of $\ln(k_{-1}/k_3)$ against $1/RT$ for isobutane dehydrogenation and cracking over Ga/HZSM-5.

for isobutane reactions over HZSM-5, and indicates that the relative reaction rate, between cracking and dehydrogenation, is controlled by the preexponential factors. Intrinsic rate parameters for the cracking and dehydrogenation reaction step can be estimated from reported adsorption enthalpies and from typical desorption preexponential factors. The enthalpy of adsorption of isobutane on HZSM-5 and silicate has been measured using a range of techniques and found to be $-48.7 \pm 4.7 \text{ kJ mol}^{-1}$ [15]. Typical preexponential factors for physisorbed systems are $A_{-1} = 10^{12 \pm 1} \text{ s}^{-1}$ [16]. From the intrinsic rate parameters listed in Table III, it may be seen that for Ga/HZSM-5 the cracking preexponential factor is larger than the dehydrogenation value by (2.1 ± 1.7) . It has been previously noted that a factor of three between preexponential factors can be associated with differences in reaction path degeneracy. For cracking of isobutane three identical C—C bonds

are available for Lewis acid attack, while only one hydrogen atom, attached to the tertiary carbon, is available for hydride abstraction. A difference in the kinetics is that the activation energies over Ga/HZSM-5 are 23 kJ mol^{-1} less than over HZSM-5, while preexponential factors are a factor of 10 larger. Smaller activation energies disagree with reported observations that gallium decreases the acid strength of the HZSM-5 active sites [17], but the increased number of Lewis acid sites [6] may contribute to a lowering of the energy barrier.

Two explanations for the large preexponential factors have previously been suggested [4]. One is that the coverage of isobutane on the external surface of the catalyst is greater than the coverage in the micropores. That is, preexponential factors for unimolecular reactions where the entropy difference between the reactant and transition-state is negligible are typically 10^{13} s^{-1}

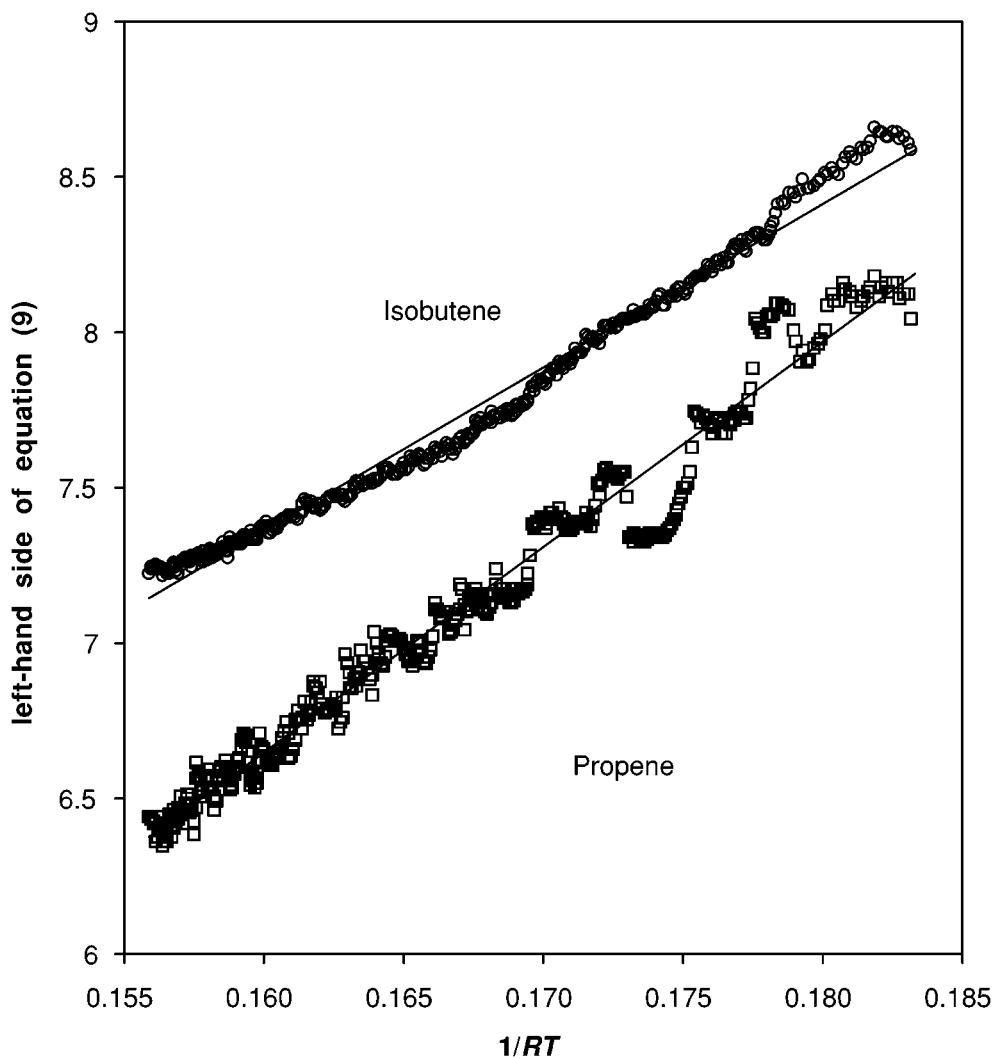


Figure 8 Arrhenius-type plots of $\ln(k_{-1}/k_3)$ against $1/RT$ for isobutane dehydrogenation and cracking over Zn/HZSM-5.

[18]. Units for the intrinsic preexponential factors listed in Table III are degrees centigrade geometric surface coverage per active site coverage. Hence, if A_{2a} or A_{2b} is much larger than 10^{13} then active site coverage \ll geometric surface coverage. It has been previously estimated that the time constant for diffusion to active sites at 200–500°C is in the range 10^{-7} – 10^{-10} s, which is much shorter than the residence time in the cell and the reaction time constants [4]. There may, however, be blockages within the zeolite or inaccessible active sites that slow the diffusion rate. A second possibility is that there is a large entropy increase when forming the transition-state. As alkanium ion formation is the dominant pathway for Ga/HZSM-5 catalyzed decomposition, entropy increase can be associated with extra vibrational motions caused by the insertion of the proton from Bronsted acid sites into the activated complex.

Cracking, Dehydrogenation, and Aromatization over Zn/HZSM-5

Fractional yields and decomposition plotted in Fig. 5 show that propene and methane formation and isobutane loss increase exponentially over the temperature range. Isobutene formation rate slows from 440°C, which shows that the dehydrogenation mechanism and hence rate are different from the cracking kinetics.

As aromatic yields are much lower than for Ga/HZSM-5, trends in these data are ambiguous. The expected statistical distribution of two toluene molecules for each benzene and xylene is not observed. By again assuming that propene and isobutene formation is a precursor to aromatic formation, cracking and dehydrogenation rate parameters are corrected by adjusting $\alpha_{\text{Product}}/I_{\text{Product}}$ using Eq. (10) and the equivalent for isobutene. Corrected activation energies and

preexponential factors were listed in Table III. Because of the small aromatic yields the rate parameters are not significantly affected by this adjustment.

Intrinsic activation energies for cracking were 13 ± 2 kJ mol⁻¹ higher than for dehydrogenation over Zn/HZSM-5 and preexponential factors varied by a factor of (20 ± 2) . Unlike for pure HZSM-5 and Ga/HZSM-5, both rate parameters controlled the relative rates of cracking and dehydrogenation of isobutane with the Zn²⁺ exchanged HZSM-5. This is further evidence that either different mechanisms or different rate determining steps are involved for the two reaction pathways. The very small rates of methane formation for this catalyst suggest that cracking, at least, is dominated by Lewis acid attack.

In comparison with Ga/HZSM-5 isobutane reactions, activation energies were significantly lower for Zn/HZSM-5; 33 ± 3 kJ mol⁻¹ and 47 ± 2 kJ mol⁻¹ for cracking and dehydrogenation respectively. Ono and Kanae [19] have shown that Zn/HZSM-5 has weaker acid sites than Ga/HZSM-5, which is an apparent contradiction to the activation energies listed in Table III. However, our results show that overall yields of all products are lower for Zn/HZSM-5, which is reflected in the significantly lower preexponential factors. Differences between intrinsic activation energies obtained for pure HZSM-5, Ga/HZSM-5 and Zn/HZSM-5 catalysts may therefore be attributed to the ratio of Lewis acid to Bronsted acid sites.

Two possible explanations for the intrinsic preexponential factors for Zn/HZSM-5 cracking and dehydrogenation, which are small when compared to Ga/HZSM-5 and pure HZSM-5 values, are proposed:

- (i) The active surface area coverage is similar to the external surface area coverage. Hamid et al. [20] observed that ion-exchanged Ga³⁺ initially tends to concentrate on the outer surface of HZSM-5, but reductive reaction and oxidative regeneration leads to a redistribution of gallium in the zeolite. Because of the smaller coordination sphere of Zn²⁺, ion exchange of this divalent cation occurs directly onto intrazeolite sites [9]. Such a distribution may allow reactants and products to more freely diffuse into the micropores of Zn/HZSM-5, and so more rapidly reach a steady-state. External Ga³⁺ may block or hinder diffusion into the micropores. Similar blockages are not expected for pure HZSM-5, but acid sites not associated with metal cations may be less accessible.
- (ii) The entropy difference between reactants and transition-state is negligible. This may be a consequence of the concentrations of Lewis and

Bronsted acid sites on the respective catalysts. Lewis acid sites may dominate for Zn/HZSM-5, while for Ga/HZSM-5 both Lewis and Bronsted acid sites contribute to the decomposition. Negligible reaction entropy differences are expected if the transition state is not larger or more complex than the reactant. For Lewis acid initiated reaction, involving hydride abstraction or electron attack of C—C bonds, the structure of the transition-state is likely to be less complex than alkanium ion formation. Continuing this argument a larger intrinsic preexponential factor for propene formation ($10^{14.8 \pm 1.1} \text{ } ^\circ\text{C}^{-1}$), when compared with isobutene ($10^{13.5 \pm 1.1} \text{ } ^\circ\text{C}^{-1}$), is consistent with a larger transition-state for cracking.

CONCLUSION

For isobutane decomposition over pure HZSM-5, Ga/HZSM-5, and Zn/HZSM-5, the dominant initial reaction pathway was cracking to form propene. Dehydrogenation was also a significant reaction, having a rate constant two to three times lower than the competing cracking reaction step. Activation energies were similar for cracking and dehydrogenation on the same catalyst for HZSM-5 and Ga/HZSM-5, and so the difference in rate was primarily due to differences in reaction path degeneracy. For isobutane catalysis on Zn/HZSM-5 a large difference in preexponential factors and activation energies were calculated for the competing reaction steps, which suggested a pathway other than alkanium ion formation is initiating decomposition.

The low rates of methane evolution over both Ga/HZSM-5 and Zn/HZSM-5 indicate that Lewis acid sites initiate cracking and dehydrogenation. That is, electron attack of C—C bonds and hydride abstraction are the primary reaction steps leaving hydrogen and methyl groups directly bonded to the catalyst surface. At low pressures and hence low coverages, bimolecular formation of H₂ and CH₄ is likely to be limited. Bronsted acid sites also contributed to isobutane decomposition, but for Zn/HZSM-5 this reaction pathway was minor. Differences between intrinsic activation energies over different catalysts reflect the ratio of the two types of acid sites on the surface.

Differences in intrinsic preexponential factors may be related to entropy differences between the reactant and transition-state. For Lewis acid attack entropy differences were small, while the formation of alkanium ions resulted in a large entropy change. An alternative explanation for the preexponential factors for isobutane

decomposition is that the ratio of exposed-site coverage to active-site coverage is high for Ga/HZSM-5, but low for Zn/HZSM-5. Blockages caused by large Ga³⁺ ions in the micropores of the zeolite may hinder the rate at which a steady-state coverage is reached.

The formation of aromatics was more prolific on Ga/HZSM-5 than on Zn/HZSM-5 at low isobutane pressures during temperature-programming. This was simply a consequence of the higher alkene yields over Ga/HZSM-5. All experiments verified that precursors to benzene, toluene and xylene were propene and isobutene or corresponding alkenium ions.

Yanping Sun is appreciative of UNERS and OPRS awards.

BIBLIOGRAPHY

1. Giannetto, G.; Monque, R.; Galiasso, R. *Catal Rev-Sci Eng* 1994, 36, 271.
2. O'Connor, C. T. In *Handbook of Heterogeneous Catalysis*; Ertl, G.; Knozinger, H.; Weitkamp, J. (Eds.); VCH: Weinheim, 1997, Vol. 4, pp. 2069.
3. Raichle, A.; Moser, S.; Traa, Y.; Hunger, M.; Weitkamp, J. *Catal Commun* 2001, 2, 23.
4. Yanping, S.; Brown, T. C. *J Catal* 2000, 194, 301.
5. Guisnet, M.; Gnep, N. S. *Appl Catal* 1996, 146, 33.
6. Kwak, B. S.; Sachtler, W. M. H. *J Catal* 1994, 145, 456.
7. Rojasova, E.; Smieskova, A.; Hudec, P.; Zidek, Z. *React Kinet Catal Lett* 1999, 66, 91.
8. Biscardi, J. A.; Iglesia, E. *J Catal* 1999, 182, 117.
9. Biscardi, J. A.; Iglesia, E. *Catal Today* 1996, 31, 207.
10. Iczkowski, R. P.; Margrave, J. L.; Robinson, S. M. *J Phys Chem* 1963, 67, 229.
11. Keyser, L. F.; Moore, S. B.; Leu, M.-T. *J Phys Chem* 1991, 95, 5496.
12. Underwood, G. M.; Li, P.; Usher, C. R.; Grassian, V. H. *J Phys Chem A* 2000, 104, 819.
13. Marczewski, M. *J Chem Soc, Faraday Trans 1* 1986, 82, 1687.
14. Bearez, C.; Avendano, F.; Chevalier, F.; Guisnet, M. *Bull Soc Chim France* 1984, 3, 346.
15. Nijhuis, T. A.; van-den-Broeke, L. J. P.; Linders, M. J. G.; Makkee, M.; Kapteijn, F.; Moulijn, J. A. *Catal Today* 1999, 53, 189.
16. Pitt, I. G.; Gilbert, R. G.; Ryan, K. R. *J Chem Phys* 1995, 102, 3461.
17. Choudhary, V. R.; Mantri, K.; Sivadinarayana, C. *Microporous Mesoporous Mater* 2000, 37, 1.
18. Benson, S. W. *Thermochemical Kinetics*, 2nd ed.; Wiley: New York, 1976.
19. Ono, Y.; Kanae, K. *J Chem Soc, Faraday Trans* 1991, 87, 669.
20. Hamid, S. B.; Derouane, E. G.; Demortier, G.; Riga, J.; Yarmo, M. A. *Appl Catal A* 1994, 108, 85.